Tech Science Press

Investigation of Core Loss Calculation Methods for Nanocrystalline Core in Medium Frequency Range

Yunxiang Guo[1], Cheng Lu[1,2], Feng Yu[1], Liang Hua[1] and Xinsong Zhang[1,*]

[1]College of Electrical Engineering, Nantong University, Nantong, 226019, China
[2]Nantong Research Institute for Advanced Communication Technologies, Nantong, 226019, China
*Corresponding Author: Xinsong Zhang. Email: prettypebble@163.com

Abstract: Nanocrystalline core is often adopted in high-power medium-frequency transformer, whose excitation voltage is usually a rectangular wave with an adjustable duty ratio. In this paper, several kinds of methods are proposed for core loss calculation under non-sinusoidal voltage excitation by modifying the original Steinmetz equation (OSE). Firstly, these correction methods are compared in theory, and their analytical equations under rectangular voltage with an adjustable duty ratio are deduced. Then, a hysteresis loop measurement system is established to measure the core loss density of a nanocrystalline core. Based on the measured results of the core loss density under sinusoidal voltage excitation, the coefficients of OSE for the core are fitted. Finally, core loss calculation results using the proposed correction methods under different amplitudes and duty ratios are analyzed and compared with the measured values. The results verify the correctness of the theoretical analysis, that waveform-coefficient Steinmetz equation is the most suitable method for loss calculation of nanocrystalline core in medium frequency range when the excitation voltage is a rectangular wave with an adjustable duty ratio.

Abbreviations

PET   Power electronic transformer
HPMFT   High-power medium-frequency transformer
OSE   Original Steinmetz equation
MSE   Modified Steinmetz equation
GSE   Generalized Steinmetz equation
IGSE   Improved generalized Steinmetz equation
WcSE   Waveform-coefficient Steinmetz equation

1 Introduction

With the development of the power electronic control technology, there is a significant improvement in the performance of power electronic transformer (PET). As a result, the PET has a promising prospect in the

application areas, such as the smart grid [1,2]. At the same time, for the fact that PET can operate at a high electromagnetic coupling frequency, the volume and weight of the transformers can be greatly reduced. As a result, PET is more suitable for electric locomotives [3,4], offshore wind farms [5,6], and other application fields, which have a strict demand for the transformer's volume and weight. PET is composed of the power electronic converters and the high-power medium-frequency transformer (HPMFT), where the HPMFT is used for electrical isolation and voltage transformation [7].

Core loss is an important part of the total loss of electric equipment, which is based on the electromagnetic coupling principle. Traditional silicon steel sheet, whose thickness is 0.3–0.5 mm, is often used in the power-frequency transformer. With the increase of the operating frequency, the core loss of the transformer will also increase significantly. Usually, the core of HPMFT is made by ultra-thin silicon steel sheet, ferrite, amorphous metals, and nanocrystalline strip [8,9]. Comparing to the traditional silicon steel sheet, they have a relatively low loss in high-frequency applications.

The saturation flux density of the silicon steel sheet can reach 1.8 T. Although JFE steel corporation has developed a 0.1 mm ultra-thin silicon steel sheet, its loss at high frequency is still higher than the other materials [10]. It is not suitable to use the ultra-thin silicon steel sheet in the applications where the operating frequency is greater than 1 kHz. Although the high-frequency loss of ferrite is low, its saturation flux density can only reach up to 0.5 T, which will result in a large volume of the transformers. Amorphous metals and nanocrystalline materials have a small high-frequency loss density while they also have a high saturation flux density (1.5 T and 1.2 T, respectively). By comparing the difference between the two materials, we can find that the saturation flux density of amorphous metals is slightly higher, and it is cheaper than nanocrystalline materials. However, the loss density of nanocrystalline materials at high frequency is better than amorphous metals. In a lower frequency range (less than 1 kHz), amorphous metal is the best choice for the core material of the transformer. But to achieve higher power density, the operation frequency of HPMFT should be as high as possible. At the same time, it is also necessary to consider the loss growth of the converters as the frequency increases. Therefore, HPMFT tends to work at the medium frequency range (1–10 kHz) [11].

In conclusion, to increase the power density and minimize the loss at the same time, nanocrystalline material is an ideal choice for the core of HPMFT. Phase shift control and series resonance control are two commonly used methods in PET [12,13], where the port voltage of the HPMFT is a rectangular wave with an adjustable duty ratio. Therefore, it is necessary and important to analyze the calculation methods for nanocrystalline core loss under this kind of voltage excitation. And the analysis work is meaningful for the design and optimization of HPMFT.

This paper is organized as follows: Section 2 introduces three kinds of analytical methods for core loss calculation. Section 3 analyzes and compares several correction methods based on the original Steinmetz equation (OSE) under non-sinusoidal excitation, where the equations of these correction methods for the core loss under rectangular voltage excitation with an adjustable duty ratio are deduced. Section 4 sets up a hysteresis loop measurement system to measure the core loss density of a nanocrystalline core. The coefficients of OSE for the core are fitted based on the measured results of the core loss density under sinusoidal voltage excitation. At the end of Section 4, calculation results of core loss density using the proposed correction methods under rectangular voltage excitation with different amplitudes and duty ratios are compared with the measured results to achieve the most accurate one. Section 5 gives the conclusions of this paper.

2 Analytical Calculation Methods of Core Loss

The analytical calculation methods of core loss are usually divided into 3 categories: magnetic hysteresis loss model based on physical phenomena; loss separation method based on core loss separation hypothesis; empirical equation method based on experimental data fitting.

Magnetic hysteresis loss model based on physical phenomena mainly includes the Jiles-Atherton (JA) model and Preisach model [14,15], where the JA model is based on the calculation of macroscopic energy and Preisach model is based on the statistics of the magnetic domain movement in time and space. These two models both have high precision, but the process of parameter identification is rather complicated due to the complexity of the models. As a consequence, these two models are not often used in practical engineering applications, especially in the applications under complex wave excitation in high frequency.

The loss separation method is based on three different effects on core loss: static hysteresis loss P_h, eddy current loss P_c, extra loss P_e. Core loss P_s is the sum of the three:

$$P_s = P_h + P_c + P_e \tag{1}$$

Compared with the hysteresis model, the loss separation method can simplify the analysis process of the core loss. The precision of the loss separation method was greatly improved [16] after Bertotti explained the physical significance of the additional loss.

The empirical equation method is based on experimental data fitting, and one most commonly used empirical equation is OSE:

$$P_v = Kf^{\alpha}B_m^{\beta} \tag{2}$$

where P_v is the core loss density, f is the frequency of exciting voltage, B_m is the amplitude of flux density, K, α, β are parameters related to the characteristics of the core material. Due to its simple form involving few parameters and relatively high accurate calculation precision, OSE is widely used in core loss calculation of electromagnetic equipment, such as inductors, transformers, and motors. However, the main drawback of OSE is that it is only suitable for calculation of core loss under sinusoidal voltage excitation.

3 Analysis of OSE Correction Methods under Non-Sinusoidal Excitation

3.1 OSE Correction Methods

As mentioned above, OSE can only be applied in core loss calculation under sinusoidal voltage excitation. When adopted in core loss calculation under non-sinusoidal excitation, some modifications must be made to OSE [17–20].

3.1.1 Modified Steinmetz Equation

It is assumed in modified Steinmetz equation (MSE) that core loss is related to the amplitude of flux density B_m and the change rate of flux density dB/dt, where an equivalent frequency f_{eq} is defined in Eq. (3) and it is related to dB/dt in one magnetization period T.

$$f_{eq} = \frac{2}{\Delta B^2 \pi^2} \int_0^T \left(\frac{dB}{dt}\right)^2 dt \tag{3}$$

where $\Delta B = B_{\max} - B_{\min}$, $B_{\max}$, $B_{\min}$ are the maximum and minimum value of flux density in one magnetization cycle. If the excitation voltage has no DC component, $\Delta B = 2B_m$. MSE is achieved by substituting f_{eq} into OSE, and it can be described as

$$P_v = (Kf_{eq}^{\alpha-1}B_m^{\beta})f \tag{4}$$

3.1.2 Generalized Steinmetz Equation

Generalized Steinmetz equation (GSE) is derived according to the deviation in core loss calculation under sinusoidal voltage excitation between OSE and MSE. Besides dB/dt, GSE considers that core loss is related to the instantaneous value of the flux density $B(t)$:

$$P_v = \frac{1}{T} \int_0^T k_1 \left| \frac{dB(t)}{dt} \right|^\alpha |B(t)|^{\beta-\alpha} dt \qquad (5)$$

where coefficient k_1 is defined as

$$k_1 = \frac{K}{(2\pi)^{\alpha-1} \int_0^{2\pi} |\cos\theta|^\alpha |\sin\theta|^{\beta-\alpha} d\theta} \qquad (6)$$

3.1.3 Improved Generalized Steinmetz Equation

The magnetization process of the core material is also related to the history of magnetization, where various magnetization reversal points can make a great difference in the shape of the hysteresis loop in one magnetization cycle. Improved generalized Steinmetz equation (IGSE) replaces the instantaneous value of flux density $B(t)$ in GSE with the peak-to-peak value of flux density ΔB in one magnetization period. As a result, the equation of IGSE can be described as

$$P_v = \frac{1}{T} \int_0^T k_i \left| \frac{dB(t)}{dt} \right|^\alpha |\Delta B|^{\beta-\alpha} dt \qquad (7)$$

where coefficient k_i is defined as

$$k_i = \frac{K}{(2\pi)^{\alpha-1} \int_0^{2\pi} |\cos\theta|^\alpha 2^{\beta-\alpha} d\theta} \qquad (8)$$

3.1.4 Waveform Coefficient Steinmetz Equation

In the case of the same amplitude, flux density curves in one magnetization period under non-sinusoidal and sinusoidal excitations are different. Waveform coefficient FWC is defined by the ratio between areas surrounded by the flux density curves and coordinate axis. Multiplying FWC by OSE, waveform-coefficient Steinmetz equation (WcSE) is achieved as

$$P_v = FWC \cdot Kf^\alpha B_m{}^\beta \qquad (9)$$

3.1.5 Theoretical Comparison of the Correction Methods

Core loss is related to many factors in the magnetization process, such as the change rate of the flux density $dB(t)/dt$, the instantaneous value of the flux density $B(t)$, and the history of magnetization ΔB. MSE and IGSE consider $dB(t)/dt$ and ΔB in the process of correction. GSE takes $dB(t)/dt$ and $B(t)$ into account. In summary, two of the above factors are considered in MSE, GSE, and IGSE, which does not contain all the factors in the magnetization process.

The most comprehensive reflection of the core magnetization process is the magnetization curve, which contains all the factors that may affect the core loss, such as $dB(t)/dt$, $B(t)$, ΔB, and so on. WcSE modified OSE based on the difference between the flux density curves under sinusoidal and non-sinusoidal excitation, which should theoretically be better than the above three correction methods.

3.2 Analytical Equations Derivation for Core Loss under Rectangular Voltage Excitation

When PET adopts parallel resonance control, the port voltage of HPMFT is a sine wave. The core loss of HPMFT can be directly calculated by OSE. When phase-shift control or series resonance control is used in PET, the port voltage of HPMFT is a rectangular wave with an adjustable duty ratio. Waveforms of rectangular voltage with an adjustable duty ratio and corresponding instantaneous flux density are presented in Fig. 1.
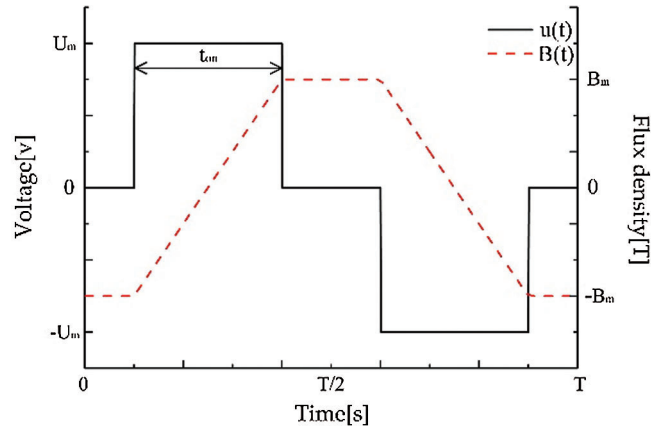
Figure 1: Waveforms of rectangular voltage and corresponding instantaneous flux density

The relationship between the amplitude of the voltage U_m and the flux density B_m is as follows:

$$U_m = \frac{4}{D} k_f n f B_m S \tag{10}$$

where k_f is the lamination coefficient of the core, n is the number of turns of the primary winding, f is the operating frequency of the transformer, S is the effective area of the magnetic circuit area. Duty ratio D of the rectangular voltage in Fig. 1 can be calculated as

$$D = \frac{2 t_{on}}{T} \tag{11}$$

where t_{on} is the time when the voltage is not zero in a half period, T is the period of the voltage.

Since IGSE is improved by GSE, this study only considers IGSE. As seen in Eqs. (3) and (7), MSE and IGSE are mainly related to the integral operation of $|dB(t)/dt|^k$ within a magnetization period, where k is a constant. The relationship between the port voltage of HPMFT $u(t)$ and the change rate of the flux density $dB(t)/dt$ is

$$u(t) = \frac{d\psi(t)}{dt} = nS \frac{dB(t)}{dt} \tag{12}$$

where $\psi(t)$ is the flux linkage. According to Eq. (12), we can get

$$\int_o^T \left| \frac{dB(t)}{dt} \right|^k dt = \frac{1}{(nS)^k} \int_0^T |u(t)|^k dt \tag{13}$$

Function expression of the rectangular voltage wave with an adjustable duty ratio is

$$u(t) = \begin{cases} 0 & (0 < t \le \frac{T}{4} - \frac{t_{on}}{2}) \\ U_m & (\frac{T}{4} - \frac{t_{on}}{2} < t \le \frac{T}{4} + \frac{t_{on}}{2}) \\ 0 & (\frac{T}{4} + \frac{t_{on}}{2} < t \le \frac{3T}{4} - \frac{t_{on}}{2}) \\ -U_m & (\frac{3T}{4} - \frac{t_{on}}{2} < t \le \frac{3T}{4} + \frac{t_{on}}{2}) \\ 0 & (\frac{3T}{4} + \frac{t_{on}}{2} < t \le T) \end{cases} \tag{14}$$

By substituting Eq. (10) and (14) into Eq. (13), we can get

$$\int_o^T \left| \frac{dB(t)}{dt} \right|^k dt = (4B_m)^k \left(\frac{f}{D} \right)^{k-1} \tag{15}$$

The key of WcSE is to calculate the waveform coefficient *FWC*. As shown in Fig. 2, the amplitudes of flux density of rectangular ($D = 0.6$) and sine voltage wave excitation are equal. By calculating the ratio of the areas surrounded by the flux density curves and the coordinate axis (presented in Fig. 2b), it can be obtained that the waveform coefficient *FWC* of the rectangular voltage wave with duty ratio D is

$$FWC = \frac{2-D}{4/\pi} = \frac{\pi}{4}(2-D) \tag{16}$$

By substituting Eq. (15) into Eq. (3) and (7), Eq. (16) into Eq. (9), the equations for core loss under rectangular voltage excitation with an adjustable duty ratio can be obtained, as shown in Tab. 1.
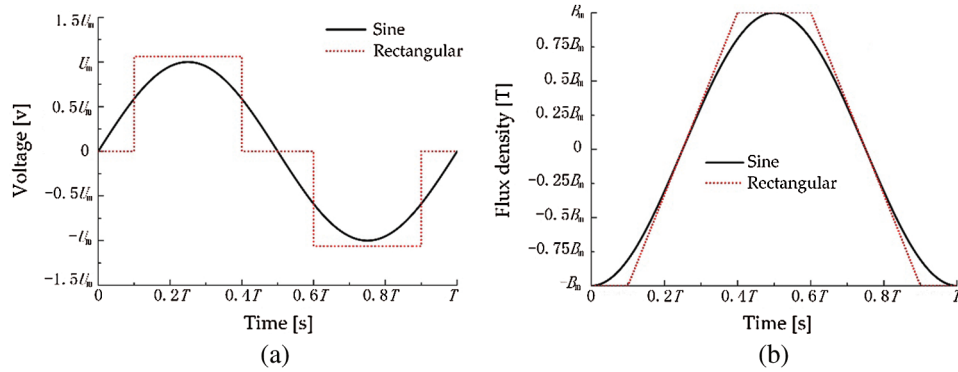

Figure 2: Waveforms of the voltage and corresponding flux density: (a) waveforms of the voltage; (b) waveforms of flux density

Table 1: Equations for core loss under rectangular voltage excitation with an adjustable duty ratio

Correction-method	Analytical equation
MSE	$\left(\dfrac{8}{\pi^2 D} \right)^{\alpha-1} k f^\alpha B_m^{\ \beta}$
IGSE	$2^{\alpha+\beta} D^{1-\alpha} k_i f^\alpha B_m^{\ \beta}$
WcSE	$\dfrac{\pi}{4}(2-D) k f^\alpha B_m^{\ \beta}$

4 Comparison of the OSE Correction Methods

4.1 Hysteresis Loop Measurement System

The hysteresis loop can not only reflect the magnetization process of the core, but also be used to calculate the core loss in the magnetization process. A hysteresis loop measurement system is built in this paper, as shown in Fig. 3. The test sample of nanocrystalline core comes from Gaotune technologies corporation.
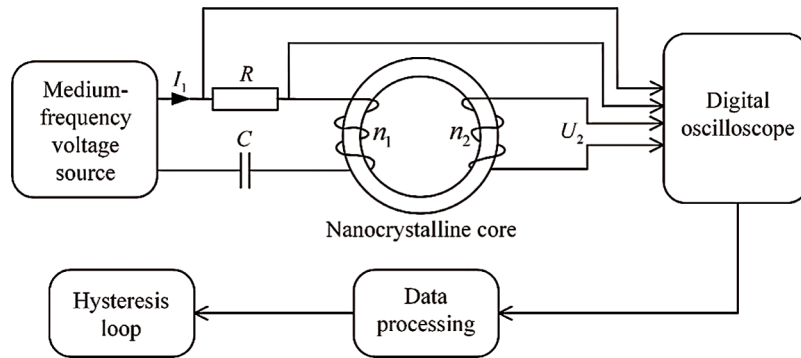
Figure 3: Measurement system for hysteresis loop of nanocrystalline core

The capacitor C in the system is the DC isolation capacitor, which is used to isolate the possible DC component in the voltage source and avoid the occurrence of magnetic bias of the core. The resistance R in the system is the sampling resistance, which is used to convert the current signal of excitation current I_1 into a voltage signal. n_1 and n_2 are respectively the turns of the primary and secondary winding, U_2 is the induced voltage of the secondary winding. Through collecting the waveform data of I_1 and U_2, and data processing by PC, the hysteresis loop of the nanocrystalline core can be drawn.

It is worth pointing out that the dynamic hysteresis loop of the core at a specific frequency is drawn by this method, which can reflect the magnetization process of the core in one magnetization cycle, and the loop area is the core loss per unit volume of the core in one magnetization cycle. The equation of the core loss per unit weight is presented as follows:

$$P_v = \rho_n f \int H dB = \rho_n f S_m \tag{17}$$

where H is the vector of magnetic field intensity, B is the vector of flux density, S_m is the area of the dynamic hysteresis loop of the core at the frequency f, ρ_n is the density of the nanocrystalline core. The area of the dynamic hysteresis loop is the larger that of the static hysteresis loop because of the eddy current loss and additional loss.

Fig. 4a shows the hysteresis loops of the nanocrystalline core under the excitation of sinusoidal voltage at various frequencies in the medium frequency band of 2–10 kHz when $B_m = 0.5$ T. Fig. 4b presents the hysteresis loops of the nanocrystalline core under the excitation of sinusoidal voltage at various flux densities when $f = 2$ kHz.
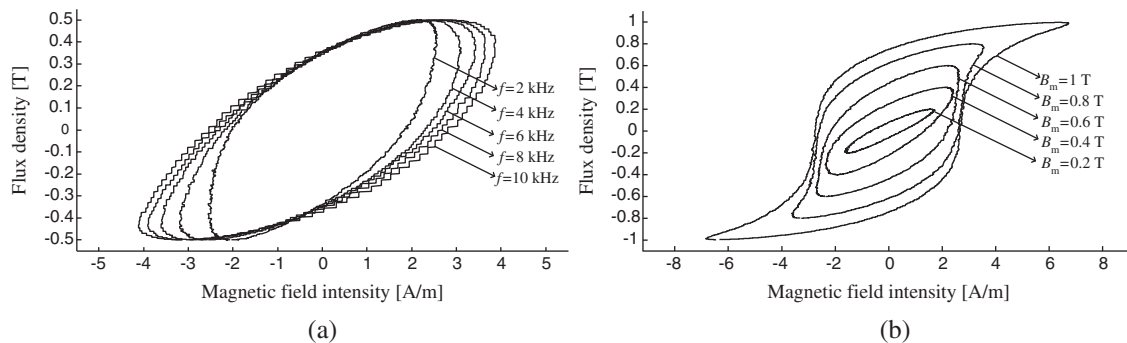

Figure 4: Hysteresis loops of the nanocrystalline core under different frequencies: (a) $B_m = 0.5$ T; (b) $f = 2$ kHz

4.2 Core Loss Calculation under Sinusoidal Voltage Excitation

Through the hysteresis loop measurement system in Fig. 3, the core loss densities of the nanocrystalline core under the sinusoidal voltage excitation are measured when f = 2–10 kHz and B_m = 0.2–1.0 T, as shown in Tab. 2.

Table 2: Core loss density of the nanocrystalline core [w/kg]

f [kHz] B_m [T]	2	4	6	8	10
0.2	0.101	0.247	0.420	0.598	0.801
0.4	0.493	1.141	1.871	2.751	3.763
0.6	2.023	2.821	4.798	6.456	9.327
0.8	2.256	5.369	8.632	13.123	17.856
1.0	3.872	9.023	14.517	21.320	27.391

Using the curve fitting toolbox in MATLAB to fit the measured results in Tab. 2, the equation of OSE for the nanocrystalline core in the above frequency range is obtained, as shown in Eq. (18).

$$P_v = 1.53 f^{1.26} B_m{}^{2.21} \tag{18}$$

4.3 Core Loss Calculation under Rectangular Voltage Excitation

By substituting the three parameters k, α, and β in the equation of OSE into the formulas in Tab. 1, the core loss calculation equations based on MSE, IGSE, and WcSE for the nanocrystalline core under the rectangular voltage excitation with an adjustable duty cycle can be obtained. In order to compare the accuracy of the three correction methods, using the hysteresis loop measurement system in Fig. 2, the rectangular voltage excitation with an adjustable duty ratio is applied to the core under the frequency of 5 kHz and the flux density amplitude of 0.2–1.0 T. The core loss density calculation values of the MSE, IGSE, and WcSE are compared with the measured results.

The core loss densities of different B_m are calculated and compared with the measured results when f = 5 kHz and D = 1, as shown in Fig. 5a. As can be seen from Fig. 5a, the results of MSE and IGSE are close and larger than the measured values. On the contrary, the results of WcSE are smaller than the measured values. Among the three correction methods, WcSE calculation curve is the closest one to the measured curve, the maximum calculation error is about 8%.

When the frequency and flux density amplitude are fixed, f = 5 kHz and B_m = 0.5 T, the core loss densities of different duty ratios under the rectangular voltage excitation are calculated. The calculation results are compared with the measured ones, which is shown in Fig. 5b. As can be seen from Fig. 5b, the smaller the duty ratio is, the greater the core loss density becomes. The results of MSE and IGSE are close, and WcSE is still the closest to the measured results. When D is small, the three correction methods have high calculation accuracy. When D is larger than 0.7, the calculation error of the three correction methods increases with the raise of D. Among the three correction methods, WcSE still has the smallest error.

When the rectangular voltage excitation has different amplitude and duty ratio, the core loss calculation results of WcSE are always the most accurate ones. The comparison results are consistent with the theoretical analysis, which is that WcSE is the most suitable method for core loss calculation of the nanocrystalline when the waveform of the excitation voltage is rectangular with an adjustable duty ratio.
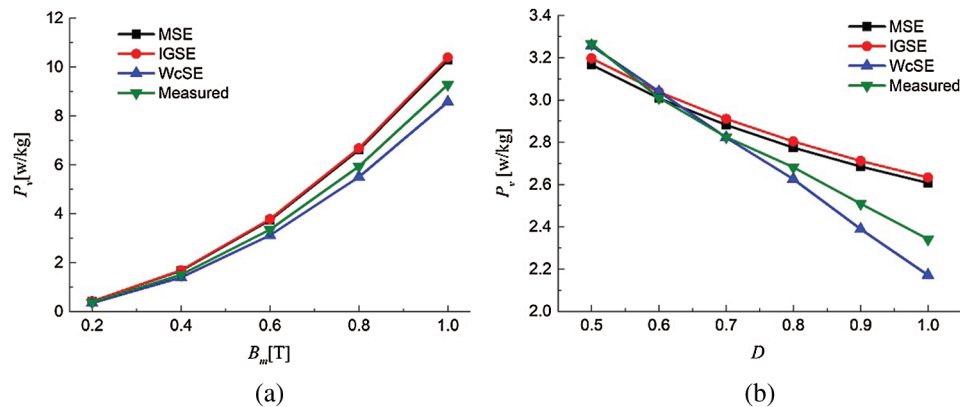
Figure 5: Core loss density: (a) core loss densities of different B_m when f = 5 kHz and D = 1; (b) core loss densities of different D when f = 5 kHz and B_m = 0.5 T

5 Conclusions

This paper analyzes the analytical methods for core loss calculation of the medium frequency transformer. Aimed at the problem that the waveform of the excitation voltage of HPMFT in PET is usually a rectangular wave with an adjustable duty ratio, several OSE-based correction methods for core loss calculation are proposed and theoretical compared. The analytical equations of these correction methods for core loss under this kind of voltage excitation are derived. A hysteresis loop measurement system is built to measure the core loss density of a nanocrystalline core. Based on the measured results of the core loss density under sinusoidal voltage excitation, the coefficient of OSE for the nanocrystalline core are fitted. On this basis, the analytical and measured results of the core loss density are compared at different flux density amplitude and duty ratio. It is found that the calculation results of WcSE are the closest to the measured results, which is consistent with the theoretical analysis. Among all the correction methods, WcSE not only has the most concise analytical expression, but also has the highest core loss calculation accuracy. When PETs using phase-shift or series resonance control, the port voltage of HPMFT is a rectangular wave with an adjustable duty ratio, WcSE is the most suitable method for core loss calculation of HPMFT.

Conflicts of Interest: The authors declare that they have no conflicts of interest to report regarding the present study.

References

1. Andresen, M., Raveendran, V., Buticchi, G., Liserre, M. (2018). Lifetime-based power routing in parallel converters for smart transformer application. *IEEE Transactions on Industrial Electronics, 65(2),* 1675–1684. DOI 10.1109/TIE.2017.2733426.
2. Ferreira Costa, L., De Carne, G., Buticchi, G., Liserre, M. (2017). The smart transformer: a solid-state transformer tailored to provide ancillary services to the distribution grid. *IEEE Power Electronics Magazine, 4(2),* 56–67. DOI 10.1109/MPEL.2017.2692381.

3. Yang, J., Liu, J., Zhang, J., Zhao, N., Zheng, T. Q. (2018). *Research on different balance control strategies for a power electronic traction transformer. IEEE Applied Power Electronics Conference and Exposition,* pp. 1821–1828.

4. Dujic, D., Zhao, C., Mester, A., Steinke, J. K., Weiss, M. et al. (2013). Power electronic traction transformer-low voltage prototype. *IEEE Transactions on Power Electronics, 28(12),* 5522–5534. DOI 10.1109/TPEL.2013.2248756.

5. Zhang, L., Zhang, D., Shui, H., Yuan, Y., Pei, Q. et al. (2017). Optimization design of medium frequency transformer for the offshore dc grid based on multi-objective genetic algorithm. *IET Power Electronics, 10(15),* 2157–2162. DOI 10.1049/iet-pel.2017.0309.

6. Bahmani, M. A., Thiringer, T., Rabiei, A., Abdulahovic, T. (2016). Comparative study of a multi-MW high-power density DC transformer with an optimized high-frequency magnetics in all-DC offshore wind farm. *IEEE Transactions on Power Delivery, 31(2),* 857–866. DOI 10.1109/TPWRD.2015.2494883.

7. Huang, P., Mao, C., Wang, D., Wang, L., Duan, Y. et al. (2017). Optimal design and implementation of high-voltage high-power silicon steel core medium-frequency transformer. *IEEE Transactions on Industrial Electronics, 64(6),* 4391–4401. DOI 10.1109/TIE.2017.2674591.

8. Shuai, P., Biela, J. (2017). Influence of material properties and geometric shape of magnetic cores on acoustic noise emission of medium-frequency transformers. *IEEE Transactions on Power Electronics, 32(10),* 7916–7931. DOI 10.1109/TPEL.2016.2636572.

9. Vaisambhayana, S., Dincan, C., Shuyu, C., Tripathi, A., Haonan, T. et al. (2016). *State of art survey for design of medium frequency high power transformer. Asian Conference on Energy, Power and Transportation Electrification,* pp. 1–9.

10. Takashi, D., Hironori, N. (2012). *High silicon steel sheet realizing excellent high frequency reactor performance. Twenty-Seventh Annual IEEE Applied Power Electronics Conference and Exposition,* pp. 1740–1746.

11. Wang, R., Xiao, F., Zhao, Z., Shen, Y., Yang, G. (2014). Effects of asymmetric coupling on winding AC resistance in medium-frequency high-power transformer. *IEEE Transactions on Magnetics, 50(11),* 1–4.

12. Gu, C., Zheng, Z., Xu, L., Wang, K., Li, Y. (2016). Modeling and control of a multiport power electronic transformer (PET) for electric traction applications. *IEEE Transactions on Power Electronics, 31(2),* 915–927. DOI 10.1109/TPEL.2015.2416212.

13. Wang, X., Liu, J., Ouyang, S., Xu, T., Meng, F. et al. (2016). Control and experiment of an H-bridge-based three-phase three-stage modular power electronic transformer. *IEEE Transactions on Power Electronics, 31(3),* 2002–2011. DOI 10.1109/TPEL.2015.2434420.

14. Liu, S. T., Huang, S. R., Chen, H. W. (2007). Using TACS functions within EMTP to set up current-transformer model based on the jiles-atherton theory of ferromagnetic hysteresis. *IEEE Transactions on Power Delivery, 22(4),* 2222–2227. DOI 10.1109/TPWRD.2007.905809.

15. Bernard, Y., Mendes, E., Bouillault, F. (2002). Dynamic hysteresis modeling based on Preisach model. *IEEE Transactions on Magnetics, 38(2),* 885–888. DOI 10.1109/20.996228.

16. Bertotti, G. (1988). General properties of power losses in soft ferromagnetic materials. *IEEE Transactions on Magnetics, 24(1),* 621–630. DOI 10.1109/20.43994.

17. Reinert, J., Brockmeyer, A., De Doncker, R. W. A. A. (2001). Calculation of losses in ferro- and ferri-magnetic materials based on the modified Steinmetz equation. *IEEE Transactions on Industry Applications, 37(4),* 1055–1061. DOI 10.1109/28.936396.

18. Jieli, L., Abdallah, T., Sullivan, C. R. (2001). *Improved calculation of core loss with nonsinusoidal waveforms. 36th IAS Annual Meeting Conference Record of the 2001 IEEE Industry Applications Conference,* pp. 2203–2210.

19. Venkatachalam, K., Sullivan, C. R., Abdallah, T., Tacca, H. (2002). *Accurate prediction of ferrite core loss with nonsinusoidal waveforms using only Steinmetz parameters. IEEE Workshop on Computers in Power Electronics Proceedings,* pp. 36–41.

20. Shen, W., Wang, F., Boroyevich, D., Tipton, C. W. (2008). Loss characterization and calculation of nanocrystalline cores for high-frequency magnetics applications. *IEEE Transactions on Power Electronics, 23(1),* 475–484. DOI 10.1109/TPEL.2007.911881.